Faecalibacterium prausnitzii Treatment Improves Hepatic Health and Reduces Adipose Tissue Inflammation in High-fat Fed Mice

Eveliina Munukka[1,2*], Anniina Rintala[1,2*], Raine Toivonen[1], Matts Nylund[3], Baoru Yang[3], Anna Takanen[5], Arno Hänninen[1,2], Jaana Vuopio[1], Pentti Huovinen[1], Sirpa Jalkanen[1,5], Satu Pekkala[1,4#]

[1] Department of Medical Microbiology and Immunology, University of Turku, Turku, Finland

[2]Department of Medical Microbiology and Immunology, Diagnostic and Related Services of Turku University Hospital, Turku, Finland

[3]Food Chemistry and Food Development, Department of Biochemistry, University of Turku, Turku, Finland

[4] Department of Health Sciences, University of Jyväskylä, Jyväskylä, Finland

[5] Medicity Research Laboratory, University of Turku, Turku, Finland

*These authors contributed equally to this work.

[#]**Correspondence** (including reprint requests) to:

Satu Pekkala, Ph.D., Department of Health Sciences, University of Jyväskylä, PO Box 35, FI-40014 University of Jyväskylä, Finland, Tel.:+358 45 358 28 98, Fax: +358 14 2602011, email: satu.p.pekkala@jyu.fi

Subject category: Microbe-microbe and microbe-host interactions

Conflicts of interest: The authors declare no conflict of interest.

ABSTRACT

Faecalibacterium prausnitzii is considered as one of the most important bacterial indicators of a healthy gut. We studied the effects of oral *F. prausnitzii* treatment on high-fat fed mice. Compared to the High-fat Control mice, *F. prausnitzii*-treated mice had lower hepatic fat content, AST and ALT, and increased fatty-acid oxidation and adiponectin signaling in liver. Hepatic lipidomic analyses revealed decreases in several species of triacylglycerols, phospholipids and cholesteryl esters. Adiponectin expression was increased in the visceral adipose tissue and the subcutaneous and visceral adipose tissues were more insulin sensitive and less inflamed in *F. prausnitzii*-treated mice. Further, *F. prausnitzii* treatment increased muscle mass that may be linked to enhanced mitochondrial respiration, modified gut microbiota composition and improved intestinal integrity. Our findings show that *F. prausnitzii* treatment improves hepatic health and decreases adipose tissue inflammation in mice and warrant the need for further studies to discover its therapeutic potential.

INTRODUCTION

Faecalibacterium prausnitzii is considered as one of the most important bacterial indicators of a healthy gut. It is the dominant member of *Clostridium leptum* subgroup accounting for more than 5% of the total gut microbiota in healthy humans (Lay et al., 2005, Flint et al., 2012). The health beneficial effects of *F. prausnitzii* stem from its' ability to produce butyrate, which favorably modulates intestinal immune system, oxidative stress and colonocyte metabolism (Hamer et al., 2008, Hamer et al., 2009). In addition, *F. prausnitzii* has been shown to secrete anti-inflammatory compounds, such as salicylic acid to its surrounding environment (Miquel et al., 2015, Quevrain et al., 2015). Besides, *F. prausnitzii* produces a microbial anti-inflammatory molecule, MAM-protein with anti-inflammatory properties that is suggested to alleviate colitis *in vivo* and to decrease activation of nuclear factor-κB signaling (Quevrain et al., 2016). Recently, a number of studies have associated a decreased abundance of this bacterium in the gut with several human diseases. Among others, the low levels of *F. prausnitzii* have been detected in inflammatory bowel disease, celiac disease, obesity and diabetes (reviewed in (Miquel et al., 2013), all of which are characterized either by food intolerance, inadequate calorie intake and/or abnormal energy metabolism.

As a proof of its anti-inflammatory properties, *F. prausnitzii* strain A2-165 has been shown to reduce colitis and inflammatory bowel disease in a mouse model (Rossi et al., 2016, Sokol et al., 2008). Similarly, *F. prausnitzii* A2-165 increased ovalbumin-specific T cell proliferation and reduced the number of IFN-γ^+ T cells *in vitro* (Rossi et al., 2016). In addition, we have found in humans that hepatic fat content >5% was associated with low *F. prausnitzii* abundance and increased adipose tissue inflammation independent of weight (Munukka et al., 2014). Hepatic fat accumulation may lead to non-alcoholic fatty liver disease (NAFLD) that is the hepatic manifestation of the metabolic disorders and highly frequent in obese individuals (Pereira et al., 2015).

By far, most of the studies described above have evaluated the effects of *F. prausnitzii* A2-165 strain on the host, while the properties of ATCC® 27766™ strain have been scarcely studied. In one study *F. prausnitzii* ATCC® 27766™ culture supernatant was found to exert protective effects on colitis in mice, probably *via* inhibition of Th17 differentiation, IL-17A secretion, by downregulating IL-6 and by upregulating IL-4 (Huang et al., 2016). Therefore, in this work we were interested in determining more profoundly the effects of ATCC® 27766™ strain on mice physiology.

MATERIALS AND METHODS

In vitro cultures

F. prausnitzii ATCC® 27766™ pure cultures were maintained at +37°C on yeast extract, casitone, fatty acid and glucose (YCFAG) agar plates (modified from (Lopez-Siles et al., 2012) in Whitley A35 anaerobic workstation (Don Whitley Scientific, UK). The cell solutions for the intragastric inoculation were prepared by suspending the cultured bacterial cells in PBS at an approximated cell density of 9×10^8 CFU/ml. The volume of a single inoculum, including ~ 2×10^8 bacterial cells, was 220 µl. The suspensions were prepared at the anaerobic atmosphere using anaerobic PBS, and the dosing syringes were sealed with parafilm to enable the viability of the bacteria prior to the inoculation.

Animals

All animal experiments were approved by the national ethics committee of animal experimentation in Finland (license: ESAVI/7258 /04.10.07/2014). 7-weeks old C57BL/6N female mice were purchased from Charles River laboratories, Europe. At the age of 8-weeks they were randomly divided in control high-fat diet (HFD), control chow and *F. prausnitzii*-treatment groups (n=6/group, 3 mice/cage) and were housed in IVC racks under SPF conditions. During the treatment period one mouse from HFD Control and one from *F. prausnitzii*-treatment group had to be excluded due to significant weight loss. The mice received food and water *ad libitum* and were maintained on a 12/12-hour light/dark cycle. The irradiated HFD (HFD, 58126 DIO Rodent Purified Diet w/60% energy) and the matching irradiated chow diet (58124 DIO Rodent Purified Diet w/10% energy) were purchased from Labdiet/Testdiet, UK. ~ 2×10^8 *F. prausnitzii* (*F. prausnitzii*-treated group) cells in PBS or PBS (Control groups) were inoculated intragastrically twice a week every two weeks. The body weight was measured in electronic scale (d=0.01 g) at the same time of day every week. Food intake was monitored at four different time points by weighing the consumed food in 24-hour period.

Tissue collections, blood analyses and liver AST and ALT analyses

After the 13-weeks treatment the overnight fasted mice were anesthetized and blood was drawn by puncturing the heart. Serum glucose and glycerol were analysed using the KONELAB 20XTi analyser (Diagnostic Products Corporation, Los Angeles, CA, USA). The subcutaneous and visceral adipose tissue, liver and *gastrocnemius* muscle were harvested, weighed with electronic scale (d=0.01 g), immersed in liquid nitrogen and stored at -80ºC. For the subsequent analyses of protein and gene expression, as well as fat content measurements, the tissues were pulverized in liquid nitrogen to obtain a homogeneous mixture of whole tissues. To analyze aspartate aminotransferase (AST) and alanine aminotransferase (ALT), ~20 mg of pulverized livers were homogenized in ice-cold lysis buffer (10 mM Tris-HCl, 150 mM $NaCl_2$, 2 mM EDTA, 1% Triton X-100, 10% glycerol and 1 mM DTT), supplemented with protease and phosphatase inhibitors (Sigma Aldrich, St Louis, USA) using TissueLyzer (Qiagen, Valencia, CA, USA). After centrifugation at 12.000 x g, AST and ALT were measured from soluble liver protein extracts with KONELAB 20XTi analyser.

Extraction and isolation of liver lipids

The lipids were isolated by a variation of the Folch method (FOLCH et al., 1957). Total lipids were extracted from ~30 mg pulverized liver by 2.5 mL Chloroform:Methanol ($CHCl_3$:MeOH) (2:1, v/v), vortexed before and after addition of 0.8 mL water with 0.88 % KCl. After centrifugation at 2000 x g for 3 min the lower $CHCl_3$-rich phase was saved, and 2 mL $CHCl_3$:MeOH (86:14, v/v) was added to the upper phase and the procedure repeated. Thereafter, the $CHCl_3$-rich phased was pooled and evaporated to dryness under nitrogen. The triacylglycerol (TAG), phospholipid (PL) and cholesteryl ester (CE) fractions were isolated using a solid-phase extraction procedure with pre-conditioned Sep-Pak Vac 6cc Silica cartridges (Waters, Dublin, Ireland). After elution of cholesteryl esters with hexane:methyl tert-butyl ether (MtBE) (200:0.8, v/v), the TAG fraction was eluted with hexane:MtBE (96:4, v/v), the column was conditioned with hexane:acetic acid (100:0.2, v/v) and MtBE:acetic acid (100:0.2, v/v), and finally the phospholipid fraction was eluted with MeOH:MtBE:H_2O (32:5:2, v/v/v). The initial extraction solvent contained the internal standards triheptadecanoin (Larodan Fine Chemicals, Malmö, Sweden), dinonadecanoyl-phosphatidylcholine (Larodan Fine Chemicals, Malmö, Sweden) and cholesteryl pentadecanoate (Nu-Check-Prep, Elysian, MN, USA).

Preparation and gas chromatography analysis of Fatty acid methyl esters

The fatty acids were analyzed as methyl esters, prepared by the sodium methoxide-catalyzed transesterification method (Christie, 1982) and analyzed with a Shimadzu GC-2010 gas chromatograph equipped with an AOC-20i auto injector and a flame ionization detector. A wall coated open tubular DB-23 column (60 m x 0.25 mm i.d., d_f 0.25 µm, Agilent Technologies, J.W. Scientific, Santa Clara, CA) was used. The program used to separate the fatty acid methyl esters had an initial oven temperature of 130 °C for 1 min, increased to 170 °C (6.5 °C/min), further increased to 220 °C (2.5 °C/min) held for 14.5 min, and finally increased to 230 °C (60 °C/min) and held for 3 min. The detector temperature was 280 °C, and the injector temperature was 270 °C. The injection volume was 1 µL. Peak identification and FAME response factors was based on the FAME 37 reference mixture (Supelco, Bellefonte, PA, USA) and quantification was done in relation to the internal standards

Histological and immunohistochemical analyses

For immunohistochemical staining 5 µm thick frozen liver sections were cut on a cryomicrotome (Leica CM 3000) at -24°C. Hematoxylin & Eosin (H&E) and Oil Red O staining were performed as previously described (Weston et al., 2015). In addition, aceton-fixed liver tissues were stained with Cy3-conjugated anti-smooth muscle actin (Sigma C6198, 1:200).

Adipose tissues were fixed in Tris-buffered zinc fixative (2.8 mM calcium acetate, 22.8 mM zinc acetate, 36.7 mM Zinc chloride in 0.1 M Tris-buffer, pH 7.4). After paraffin and endogenous peroxidase removal the sections were stained using Vectastain Elite ABC kit (PK-6104 Vector Laboratories) according to manufacturer's instructions. The first stage antibody was anti-mouse CD45 (clone 30F11, BD 553076) 1 µg/ml (overnight at +4°C) or negative control antibody. Diaminobenzedine (DAKO) was used as a chromogen and the sections were counterstained using Mayer's hematoxylin.

Gene and protein expression analyses

Real-time quantitative PCR and Western blot were performed as previously described by us (Pekkala et al., 2015). Real-time PCR analysis was done according to MIQE guidelines using

in-house designed primers (from Invitrogen), iQ SYBR Supermix and CFX96™ Real-time PCR Detection System (Bio-Rad Laboratories, Richmond, CA, USA). The sequences of the primers used in qPCR are presented in Supplementary table 1. Western blots were done with primary antibodies from Cell Signaling Technology (Danvers, MA, USA), and by scanning the blots using Odyssey CLX Infrared Imager of Li-COR and Odyssey anti-rabbit IRDye 800CW and anti-mouse IRDye 680RD (LI-COR Biosciences, Lincoln, NE, USA) as secondary antibodies. The quantified bands were normalized to two Ponceau S-stained bands due to that there were differences in the levels of housekeeping proteins between the groups.

DNA extraction from stools and colon content

Stool samples were collected before the treatments and frozen in liquid nitrogen. Following the sacrification, the colon and cecum content was collected and frozen in liquid nitrogen. The samples were stored at -75°C until further use. The microbial DNA was extracted from ~100 mg of the frozen samples with GXT Stool Extraction Kit VER 2.0 (Hain Lifescience GmbH, Germany) combined with an additional homogenization by bead-beating in 1.4 mm Ceramic Bead Tubes with MO BIO PowerLyzer™ 24 Bench Top Bead-Based Homogenizer (MO BIO Laboratories, Inc., CA, USA). The DNA concentrations of the extracts were measured with Qubit 2.0 fluorometer (Life Sciences), and the DNAs were stored at -75°C.

Gut microbiota composition analysis

The microbiota composition of stool and gut content were analyzed with Illumina MiSeq next generation sequencing approach. The 16S rRNA gene libraries were generated in a single PCR with the custom-designed dual-indexed primers containing the adapter and specific index sequences required for sequencing. The approach is described in Supplemental methods.

Statistics

All data were checked for normality using the Shapiro-Wilk´s test in PASW 18.0 for Windows. Due to a small sample size and that most of the data was not normally distributed,

the group differences in gene expression, protein phosphorylation levels, liver triglyceride content, and variables related to body composition and the numbers of leukocytes were analyzed by non-parametric tests using IBM SPSS Statistics 22. First, differences between the groups were analyzed using Kruskal-Wallis (for k samples) and second, the difference was identified and statistical significance determined using Mann-Whitney U test. The group differences in the gut microbiota composition were analyzed by the non-parametric Kruskal-Wallis test using JMP Pro 11 (SAS) and the statistical tools of QIIME pipeline. Taxonomic levels L2 (phyla) and L6 (genera) were studied.

RESULTS

Faecalibacterium prausnitzii treatment improves hepatic AST and ALT, lipid profile, and enhances adiponectin signaling and lipid oxidation in mice liver

C57BL/6 mice on a high-fat diet (HFD) are widely used as a model for obesity and hepatic diseases (Takahashi et al., 2012). The HFD mice were treated with *F. prausnitzii* to study the effects of the bacterium on the host health and metabolism. The results were compared to those of mice on HFD (Control HFD) and chow diet (Control chow). The study outline and weight gain during the experiment are presented in Supplementary figure S1A and B, respectively. In the *F. prausnitzii*-treated mice weight gain was higher than in the Control

chow group during weeks 1 to 4 and week 10 (p= 0.017, 0.004, 0.004, 0.004 and 0.009, respectively).

Compared to Control HFD, *F. prausnitzii*-treated mice had significantly lower hepatic AST (p=0.029) and ALT (p=0.029) values, and the Control Chow lower ALT (Figure 1A). The Oil Red O-staining of liver sections confirmed the consequences of high fat diet. Moreover, this was accompanied with ballooning and bright α-smooth muscle actin staining (Figure 1B). The mice treated with *F. prausnitzii* had significantly less triglycerides in liver (p=0.029) compared to the Control HFD mice (Figure 1C).

Gas chromatography analyses of hepatic lipid classes revealed a decrease in *F. prausnitzii*-treated mice in the molar percentages of 18:0 (stearate), 20:4n-6 (arachidonic acid), 20:5n-3 (eicosapentaenoic acid) and 22:6n-3 (docosahexanoic acid) in triacylglycerols (TAG) compared to the Control HFD mice (Table 1). Compared to the Control Chow group, the Control HFD mice had higher proportions of most fatty acids in TAG except 18:1n-9 (oleic acid), 20:1n-9 (eicosenoic acid) and 20:2n-6 (eicosadienoic acid) which were lower in the Control HFD mice ($p < 0.05$, Table 1). Compared to the Control HFD group the molar percentages of several fatty acids in phospholipids were decreased in the Control Chow group and the *F. prausnitzii*-treated group (Table 1). In contrast, 16:1 (palmitate), 18:1n-9, 20:2n-6 and 20:3n-6 (eicosatrienoic acid) increased in the phospholipids of the Control Chow group ($p<0.05$ for all, Table 1), and 20:2n-6 and 20:4n-6 (arachidonic acid) in the *F. prausnitzii*-treated group ($p<0.05$ for both, Table 1). For cholesteryl esters the *F. prausnitzii*-treated mice had higher proportions of 20:2n-6 and 20:3n-6 and lower levels of 16:0 and 20:1n-9 ($p < 0.05$ for all, Table 1) compared to the Control HFD group. Compared to the Control HFD group the Control Chow group had higher levels of 16:1, 18:1n-9 and 20:3n-6, and lower proportions of 16:0, 18:0, 18:2n-6 (linoleic acid), 18:3n-3 (α-linoleic acid), 20:5n-3 and 22:6n-3 ($p < 0.05$ for all, Table 1).

The reduced hepatic fat content was not due to changes in serum glycerol and glucose that are substrates of lipid synthesis (Figure S2A). In addition, no significant differences in food intake were found between the groups in long term (Supplementary figure S2B). However, at one measurement point at the beginning of the treatments, compared to the HFD Control group, the other groups consumed less food (Supplementary figure S2B).

Despite the lower triglyceride levels and fat content in the liver, the *F. prausnitzii*-treated mice and the Control chow mice expressed more triglyceride-synthesizing diacylglycerol-

acyltransferase, *DGAT2* (p=0.008 and p=0.009, respectively, Figure S3A) and fatty acid-synthesizing acetyl coenzyme carboxylase, *Acc2* (p=0.029 and p=0.016, respectively, Figure S3A) than the HFD control group. The lipid clearance in the *F. prausnitzii*-treated mice was likely increased, as these mice expressed more lipid metabolism-regulating adiponectin receptor, *AdipoR* (p=0.008, Figure 2A) and lipid-oxidizing citrate synthase, *CS* (p=0.008, Figure 2B). In addition, the *F. prausnitzii*-treated mice had more Ser79-phosphorylated Acc2 that turns the fatty acid metabolism onto oxidation instead of synthesis (p=0.048, Figure 2C) (Ha et al., 1994). In turn, less phosphorylated AS160 in the *F. prausnitzii*-treated mice compared to the HFD control group (p=0.043, Figure 2D) may indicate decreased glucose uptake for fat synthesis as AS160 promotes the translocation of GLUT4 glucose transporters to the cell membrane (Lansey et al., 2012). The expression of *CDKN1A* and *DDIT4*, whose reduced expression has been associated with fibrosis and over-active mTOR signaling, respectively (Williamson et al., 2014, Aravinthan et al., 2014) was highest in the *F. prausnitzii*-treated mice ($p<0.05$ for both, Supplementary figure S3B).

When compared to the HFD Control group, the direction of the effects of the *F. prausnitzii* treatment was almost exclusively the same as in the Chow diet except that the chow diet did not increase *CS* and *AdipoR* (Figure 2A&B) but increased insulin receptor *IRβ* (p=0.008, Supplementary figure S3C), while the *F. prausnitzii*-treated mice had a non-significant trend towards increased *IRβ* expression (p=0.09, Supplementary figure S3C).

The participation of other peripheral tissues in hepatic fat accumulation has been recognized (Lomonaco et al., 2012, Deivanayagam et al., 2008) and therefore we further studied the molecular changes in the visceral and subcutaneous adipose tissue as well as *gastrocnemius* muscles.

F. prausnitzii treatment increased adiponectin expression and insulin sensitivity, and decreased inflammation in the visceral adipose tissue

The visceral adipose tissue drains to the portal vein and therefore liver is directly exposed to e.g. adipokines secreted by this tissue (Rytka et al., 2011). Importantly, the expression of visceral fat-specific adipokine, adiponectin, that enhances fat oxidation in the liver was increased in the *F. prausnitzii*-treated mice compared to the HFD control group (*AdipoQ*, p=0.029, Figure 3A).

The increased fat mass in obesity-related metabolic disorders is associated with infiltrations of leukocytes to the adipose tissue, which subsequently exacerbates insulin resistance (Olefsky and Glass, 2010). Despite the higher visceral adipose tissue mass compared to the Control chow group ($p=0.006$, Figure 3B), compared to Control HFD group the *F. prausnitzii*-treated mice had significantly reduced number of CD45-positive leukocytes ($p=0.006$, Figure 3C) that were determined from the histological samples. Consequently, the visceral adipose tissue of the *F. prausnitzii*-treated mice was more insulin sensitive in terms of increased *IRβ* expression ($p=0.016$, Figure 3D) and insulin-responsive HSL phosphorylation ($p=0.021$, Figure 3E).

Compared to the HFD, the chow diet again resulted in similar insulin signaling-related changes as the *F. prausnitzii* treatment (Figure 3D and 3E) suggesting that the treatment was able to protect from some deleterious effects of the HFD. The circumstance that *F. prausnitzii*-treated mice had higher visceral fat mass than the Chow mice, may be explained by the fact that the Chow group likely oxidized more fat due to a higher expression of *Acc2* ($p=0.014$, Figure S4A), which also was more phosphorylated ($p=0.014$, Figure S4B).

F. prausnitzii treatment reduced inflammation and affected the phosphorylation of glucose-uptake related protein in the subcutaneous adipose tissue

It has been suggested that in obesity the glucose uptake by the adipose tissue is reduced (Virtanen et al., 2002). However, though the *F. prausnitzii*-treated mice had higher subcutaneous fat mass than the Control HFD group ($p=0.047$) and the Control chow group ($p=0.006$, Figure 4A), the treatment significantly increased AS160 phosphorylation compared to both control groups ($p<0.05$ for both, Figure 4B). Compared to the HFD control group the *F. prausnitzii*-treated mice had less CD45-positive cells ($p<0.05$, Figure 4C), which is an indication of reduced inflammation. No other major changes in response to the *F. prausnitzii* treatment were detected in the subcutaneous adipose tissue.

The control chow group expressed more *Acc2* ($p=0.016$, Supplementary figure S5A) that was more phosphorylated ($p=0.014$, Supplementary figure S5B) compared to the HFD group. In addition, compared to the HFD, the chow diet increased HSL phosphorylation ($p=0.01$).

F. prausnitzii treatment increased gastrocnemius muscle size and the expression of mitochondrial respiratory chain protein ATP5A

Recently, it has been proposed that the gut microbiota may affect muscle growth and metabolism (Bindels and Delzenne, 2013). *F. prausnitzii*-treated mice had higher muscle mass than the HFD control group (for the left *gastrocnemius* p=0.028 and for the right *gastrocnemius* p=0.009, Figure 5A). However, the expression of muscle growth-related PGC1α protein was not increased (data not shown). Compared to the HFD control group, the *F. prausnitzii*-treated mice had higher expression levels of mitochondrial respiratory chain complex subunit ATP5A (p=0.047, Figure 5B) and a tendency for higher UQCRC2 and MTCO1 expression (p=0.05 for both, Figure 5B), while no differences were found in the expression of NDUFS88 and SDHB or in the phosphorylation levels of Acc, AS160 and HSL (data not shown).

F. prausnitzii treatment changed the gut microbiota composition and increased the intestinal Tjp1 gene expression

In the stool samples collected before the treatment, no phylum level differences were seen between the treatment groups (Figure 6A), while in the samples collected after sacrification, the phylum level bacterial composition differed significantly between the groups (Figure 6B). Compared to the Control HFD group, the amount of phylum *Bacteroidetes* was significantly lower and the abundance of *Firmicutes* was significantly higher in the *F. prausnitzii*-treated mice ($p<0.05$ for both, Figure 6B). The same trend was noticed when *F. prausnitzii*-treated mice were compared to the Control Chow group (p=0.07 for both, Figure 6B). In addition, phylum *Cyanobacteria* was more abundant in Control Chow mice than in Control HFD and *F. prausnitzii*-treated mice ($p<0.05$ for both).

In the bacterial genus level, the only pre-treatment difference was the abundance of genus *Allobaculum* being higher in Control Chow mice than in Control HFD and *F. prausnitzii*treated mice ($p<0.05$ for both; Figure 6A). By contrast, several differences were seen in the post treatment colon content samples between the groups, most prominent being the increased abundances of genera *Lactobacillus* and *Streptococcus* in *F. prausnitzii*-treated mice compared to the Control HFD and Control Chow mice ($p<0.05$ for both; Figure 6B). In addition, genus *Allobaculum,* which was not prevalent in the Control HFD mice, was highly

abundant in the majority of the Control Chow mice and in all *F. prausnitzii*-treated mice ($p=0.12$ and $p<0.05$, respectively, Figure 6B).

The beneficial, anti-inflammatory bacteria have been shown to enhance intestinal barrier functions and integrity (Eun et al., 2011). Similarly, we found that compared to the HFD control group, *F. prausnitzii* treatment significantly increased the intestinal tight junction protein-encoding *Tjp1* gene expression ($p=0.043$, Supplementary figure S5A) that may indicate increased gut integrity.

DISCUSSION

In this work we found that the hepatic lipid content was lower in the *F. prausnitzii*-treated and Control Chow mice than in the HFD Control mice. The findings of the lipid measurements, histological liver samples as well as the AST and ALT of the *F. prausnitzii*-treated mice and the Control chow mice support each other and suggest that these mice had healthier liver than the Control HFD mice.

Several molecular changes may explain the lower lipid content in either *F. prausnitzii*-treated mice or the Control chow group or in both. First, in addition to absorbing circulating fatty

388 acids, hepatocytes synthesize fatty acids from dietary carbohydrates that reach the
389 hepatocytes via the portal vein (Bechmann et al., 2012). We did not find any differences in
390 food intake or blood glucose levels that would directly support a carbohydrate-dependent
391 mechanism. However, compared to the HFD control group the *F. prausnitzii*-treated mice
392 had lower phosphorylation levels of AS160 that may lead to a decrease in glucose uptake and
393 further reduced fat synthesis as the phosphorylated AS160 promotes translocation of GLUT4
394 glucose transporters to the cell membrane upon insulin stimulation (Brewer et al., 2014,
395 Wang et al., 2013). Nevertheless, we did not measure glucose uptake *in* vivo. Second, an
396 enhanced lipid clearance may have occurred due to higher expression levels of adiponectin
397 receptor and higher phosphorylation levels of acetyl coenzyme carboxylase (Acc) in both *F.*
398 *prausnitzii*-treated and chow mice. In liver, adiponectin signaling regulates both glucose and
399 lipid metabolism (Liu et al., 2012). Adiponectin receptor activates AMPK that further acts a
400 major regulator of lipid metabolism through direct phosphorylation of its substrates, such as
401 Acc (Rogers et al., 2008). Acc in turn catalyzes the pivotal step of fatty acid synthesis
402 pathway, and the phosphorylation of Acc at Ser79 inhibits the enzymatic activity of Acc
403 turning the lipid metabolism on oxidation (Ha et al., 1994). In addition, increased expression
404 of citrate synthase in the *F. prausnitzii*-treated mice may provide additional evidence of
405 enhanced fatty acid β-oxidation and lipid clearance from liver as it shuttles the fatty acid-
406 derived Acetyl CoA-moieties to the tricarboxylic acid cycle (Turner et al., 2007). Similarly,
407 an increased expression of *DDIT4* may limit hyperactive mTORC1 signaling and further
408 reduce lipogenesis (Williamson et al., 2014).

409 However, our findings about the molar percentages of some lipid classes are not completely
410 in line with reports from humans and high-fat fed mice. Jordy et al. showed that 16:0 and
411 18:0 were increased in TAG of high-fat fed mice compared to normal chow (Jordy et al.,
412 2015) while we did not find an increase in 16:0. Depletion of eicosapentaenoic and
413 docosahexanoic acid in TAG has been reported in steatosis and steatohepatosis (Puri et al.,
414 2007, Videla et al., 2004) while our results show the depletion in *F. prausnitzii*-treated and
415 Chow mice that according to histology and ALT measurements have healthier liver.
416 Nevertheless, several phospholipids were decreased compared to the Control HFD, which is
417 in agreement with the higher amount of phospholipids detected in steatosis (Videla et al.,
418 2004). In turn, eicosanoids are key mediators and regulators of inflammation and are
419 generated from 20 carbon polyunsaturated fatty acids (Calder, 2011). Notably, 20:2n-6
420 (eicosadienoic acid) was increased in phospholipids of both Chow and *F. prausnitzii*-treated

421 mice and 20:4n-6 (arachidonic acid) of *F. prausnitzii*-treated mice compared to HFD
422 Controls, and may be an indication of anti-inflammatory effects.

423 Recently, SNP rs762623 that reduces the expression of *CDKN1A* (Kong et al., 2007) has
424 been shown to associate with fibrosis in NAFLD patients (Aravinthan et al., 2014).
425 Therefore, an increased expression of *CDKN1A* in response to *F. prausnitzii* treatment may
426 be an indication of reduced hepatic fibrosis. In agreement with decreased fibrosis, hepatic
427 AST and ALT levels and α-smooth muscle actin, all markers of liver fibrosis (Naveau et al.,
428 2009, Weston et al., 2015) were lower in *F. prausnitzii*-treated and Control Chow mice.

429 The higher subcutaneous fat mass of the *F. prausnitzii*-treated mice may be explained by
430 decreased β-oxidation and increased fat deposition due to lower Acc and citrate synthase
431 levels. Generally, in obesity adipocyte hypertrophy in the expanding adipose tissue leads to
432 local hypoxia and subsequent cell death that drive leukocyte infiltration into the adipose
433 tissue ensuing increased inflammation (Kanda et al., 2006). However, despite the higher fat
434 mass, intensely decreased infiltration of CD45-positive leukocytes was observed in both *F.*
435 *prausnitzii*-treated groups, which is in agreement with the known anti-inflammatory effects of
436 this bacterium (Quevrain et al., 2015, Miquel et al., 2015).

437 In the visceral adipose tissue *F. prausnitzii* treatment increased the expression of adiponectin,
438 which, predominantly secreted by the visceral adipose tissue, has several insulin-sensitizing
439 effects at the whole organism level (Caselli, 2014). In accordance, low concentrations of this
440 adipokine have been associated with obesity, type 2 diabetes and NAFLD that are
441 characterized by insulin resistance (Meier and Gressner, 2004). A recent study shed light to
442 the possible mechanisms that connect the gut microbes to host's adiponectin signaling by
443 showing that the cell wall components of gram-positive bacteria stimulated adiponectin
444 secretion from mesenteric adipocytes, while lipolysaccharides (LPS) from gram-negative
445 bacteria inhibited the secretion (Taira et al., 2015). In agreement with the findings of Taira et
446 al. though initially *F. prausnitzii* was classified as gram-negative it resembles
447 phylogenetically more gram-positive than negative bacteria and therefore likely has similar
448 cell wall properties to gram-positive ones being able to stimulate adiponectin expression
449 (Lopez-Siles et al., 2012).

450 It has been suggested that gut microbiota may also influence muscle size and metabolism
451 (Bindels and Delzenne, 2013). Initially it was proposed that intestine-derived Fiaf could
452 increase muscular PGC1α expression, which is one of the master regulators of oxidative

453 metabolism and prevents muscles from atrophy (Backhed et al., 2007). In this study we did
454 not find any differences between the groups in PGC1α expression. However, it should be
455 noted that we only observed the endpoint situation of the treatments and it may be that at
456 some point during the muscle growth, the *F. prausnitzii*-treated mice may have displayed
457 higher expression levels. Yet, at the time of sacrification the oxidative metabolism may have
458 been enhanced as these mice expressed higher levels of mitochondrial ATP5A that forms a
459 part of the mitochondrial respiratory complex. Notwithstanding, the studies on the
460 mechanistic effects of the so-called beneficial microbes on muscles are scarce (Bindels et al.,
461 2012) and definitely are increasingly needed as for instance cancer-associated cachexia is an
462 important health problem.

463 The *F. prausnitzii* treatment caused substantial changes in the gut microbiota, especially by
464 promoting the growth of genera *Lactobacillus* and *Streptococcus*. In addition, the abundance
465 of the genus *Allobaculum* was remarkably higher in both normal chow and *F. prausnitzii*-
466 treated mice than in the HFD control group. *Allobaculum* genus consists of short-chain fatty-
467 acid producing bacteria and has been previously linked to weight reduction in mice (Ravussin
468 et al., 2012). The changes in gut microbiota composition may be linked to the increased *Tjp1*
469 expression in the *F. prausnitzii*-treated mice. In agreement, health-beneficial probiotic
470 bacteria have been shown to improve gut integrity through increased Tjp1 expression
471 (Bomhof et al., 2014).

472 In conclusion, *F. prausnitzii*-treated mice had lower hepatic fat content, fibrosis and AST and
473 ALT than mice on HFD without treatment. The related molecular changes seem to involve
474 increased fatty-acid oxidation and adiponectin signaling in liver and increased adiponectin
475 expression in visceral adipose tissue. In addition, the subcutaneous and visceral adipose
476 tissues were less inflamed and more insulin sensitive in *F. prausnitzii*-treated mice.

477

478

479

480

481

482

ACKNOWLEDGEMENTS

We thank the laboratory technicians Mervi Matero, Kaisa-Leena Tulla, Heidi Kunnasranta and Anna Aatisinki for the excellent technical assistance. This study has been financially supported by The Academy of Finland postdoctoral research fellow for Dr. Satu Pekkala (Grant ID 267719), by The Finnish Diabetes Research Foundation, by the Finnish Culture foundation (Central and Southwest Finland funds for Dr. Pekkala and Dr. Munukka, respectively), by the Turku University foundation for MSc. Rintala, by Instrumentarium Research foundation and Diabetes Wellness foundation.

REFERENCES

ARAVINTHAN, A., MELLS, G., ALLISON, M., LEATHART, J., KOTRONEN, A., YKI-JARVINEN, H., *et al.* 2014. Gene polymorphisms of cellular senescence marker p21 and disease progression in non-alcohol-related fatty liver disease. *Cell Cycle,* 13**,** 1489-94.

BACKHED, F., MANCHESTER, J. K., SEMENKOVICH, C. F. & GORDON, J. I. 2007. Mechanisms underlying the resistance to diet-induced obesity in germ-free mice. *Proc Natl Acad Sci U S A,* 104**,** 979-84.

BECHMANN, L. P., HANNIVOORT, R. A., GERKEN, G., HOTAMISLIGIL, G. S., TRAUNER, M. & CANBAY, A. 2012. The interaction of hepatic lipid and glucose metabolism in liver diseases. *J Hepatol,* 56**,** 952-64.

BINDELS, L. B., BECK, R., SCHAKMAN, O., MARTIN, J. C., DE BACKER, F., SOHET, F. M., *et al.* 2012. Restoring specific lactobacilli levels decreases inflammation and muscle atrophy markers in an acute leukemia mouse model. *PLoS One,* 7**,** e37971.

BINDELS, L. B. & DELZENNE, N. M. 2013. Muscle wasting: the gut microbiota as a new therapeutic target? *Int J Biochem Cell Biol,* 45**,** 2186-90.

BOMHOF, M. R., SAHA, D. C., REID, D. T., PAUL, H. A. & REIMER, R. A. 2014. Combined effects of oligofructose and Bifidobacterium animalis on gut microbiota and glycemia in obese rats. *Obesity (Silver Spring),* 22**,** 763-71.

BREWER, P. D., HABTEMICHAEL, E. N., ROMENSKAIA, I., MASTICK, C. C. & COSTER, A. C. 2014. Insulin-regulated Glut4 translocation: membrane protein trafficking with six distinctive steps. *J Biol Chem,* 289**,** 17280-98.

CALDER, P. C. 2011. Fatty acids and inflammation: the cutting edge between food and pharma. *Eur J Pharmacol,* 668 Suppl 1**,** S50-8.

CASELLI, C. 2014. Role of adiponectin system in insulin resistance. *Mol Genet Metab,* 113**,** 155-60.

CHRISTIE, W. W. 1982. A simple procedure for rapid transmethylation of glycerolipids and cholesteryl esters. *J Lipid Res,* 23**,** 1072-5.

DEIVANAYAGAM, S., MOHAMMED, B. S., VITOLA, B. E., NAGUIB, G. H., KESHEN, T. H., KIRK, E. P., *et al.* 2008. Nonalcoholic fatty liver disease is associated with hepatic and skeletal muscle insulin resistance in overweight adolescents. *Am J Clin Nutr,* 88**,** 257-62.

EUN, C. S., KIM, Y. S., HAN, D. S., CHOI, J. H., LEE, A. R. & PARK, Y. K. 2011. Lactobacillus casei prevents impaired barrier function in intestinal epithelial cells. *APMIS,* 119**,** 49-56.

FLINT, H. J., SCOTT, K. P., LOUIS, P. & DUNCAN, S. H. 2012. The role of the gut microbiota in nutrition and health. *Nat Rev Gastroenterol Hepatol,* 9**,** 577-89.

FOLCH, J., LEES, M. & SLOANE STANLEY, G. H. 1957. A simple method for the isolation and purification of total lipides from animal tissues. *J Biol Chem,* 226**,** 497-509.

HA, J., DANIEL, S., BROYLES, S. S. & KIM, K. H. 1994. Critical phosphorylation sites for acetyl-CoA carboxylase activity. *J Biol Chem,* 269**,** 22162-8.

HAMER, H. M., JONKERS, D., VENEMA, K., VANHOUTVIN, S., TROOST, F. J. & BRUMMER, R. J. 2008. Review article: the role of butyrate on colonic function. *Aliment Pharmacol Ther,* 27**,** 104-19.

HAMER, H. M., JONKERS, D. M., BAST, A., VANHOUTVIN, S. A., FISCHER, M. A., KODDE, A., *et al.* 2009. Butyrate modulates oxidative stress in the colonic mucosa of healthy humans. *Clin Nutr,* 28**,** 88-93.

HUANG, X. L., ZHANG, X., FEI, X. Y., CHEN, Z. G., HAO, Y. P., ZHANG, S., *et al.* 2016. Faecalibacterium prausnitzii supernatant ameliorates dextran sulfate sodium induced colitis by regulating Th17 cell differentiation. *World J Gastroenterol,* 22**,** 5201-10.

JORDY, A. B., KRAAKMAN, M. J., GARDNER, T., ESTEVEZ, E., KAMMOUN, H. L., WEIR, J. M., *et al.* 2015. Analysis of the liver lipidome reveals insights into the protective effect of exercise on high-fat diet-induced hepatosteatosis in mice. *Am J Physiol Endocrinol Metab,* 308**,** E778-91.

KANDA, H., TATEYA, S., TAMORI, Y., KOTANI, K., HIASA, K., KITAZAWA, R., *et al.* 2006. MCP-1 contributes to macrophage infiltration into adipose tissue, insulin resistance, and hepatic steatosis in obesity. *J Clin Invest,* 116**,** 1494-505.

KONG, E. K., CHONG, W. P., WONG, W. H., LAU, C. S., CHAN, T. M., NG, P. K., *et al.* 2007. p21 gene polymorphisms in systemic lupus erythematosus. *Rheumatology (Oxford),* 46**,** 220-6.

LANSEY, M. N., WALKER, N. N., HARGETT, S. R., STEVENS, J. R. & KELLER, S. R. 2012. Deletion of Rab GAP AS160 modifies glucose uptake and GLUT4 translocation in primary skeletal muscles and adipocytes and impairs glucose homeostasis. *Am J Physiol Endocrinol Metab,* 303**,** E1273-86.

LAY, C., SUTREN, M., ROCHET, V., SAUNIER, K., DORE, J. & RIGOTTIER-GOIS, L. 2005. Design and validation of 16S rRNA probes to enumerate members of the Clostridium leptum subgroup in human faecal microbiota. *Environ Microbiol,* 7**,** 933-46.

LIU, Q., YUAN, B., LO, K. A., PATTERSON, H. C., SUN, Y. & LODISH, H. F. 2012. Adiponectin regulates expression of hepatic genes critical for glucose and lipid metabolism. *Proc Natl Acad Sci U S A,* 109**,** 14568-73.

LOMONACO, R., ORTIZ-LOPEZ, C., ORSAK, B., WEBB, A., HARDIES, J., DARLAND, C., *et al.* 2012. Effect of adipose tissue insulin resistance on metabolic parameters and liver histology in obese patients with nonalcoholic fatty liver disease. *Hepatology,* 55**,** 1389-97.

LOPEZ-SILES, M., KHAN, T. M., DUNCAN, S. H., HARMSEN, H. J., GARCIA-GIL, L. J. & FLINT, H. J. 2012. Cultured representatives of two major phylogroups of human colonic Faecalibacterium prausnitzii can utilize pectin, uronic acids, and host-derived substrates for growth. *Appl Environ Microbiol,* 78**,** 420-8.

MEIER, U. & GRESSNER, A. M. 2004. Endocrine regulation of energy metabolism: review of pathobiochemical and clinical chemical aspects of leptin, ghrelin, adiponectin, and resistin. *Clin Chem,* 50**,** 1511-25.

MIQUEL, S., LECLERC, M., MARTIN, R., CHAIN, F., LENOIR, M., RAGUIDEAU, S., *et al.* 2015. Identification of metabolic signatures linked to anti-inflammatory effects of Faecalibacterium prausnitzii. *MBio,* 6.

MIQUEL, S., MARTIN, R., ROSSI, O., BERMUDEZ-HUMARAN, L. G., CHATEL, J. M., SOKOL, H.*, et al.* 2013. Faecalibacterium prausnitzii and human intestinal health. *Curr Opin Microbiol,* 16**,** 255-61.

MUNUKKA, E., PEKKALA, S., WIKLUND, P., RASOOL, O., BORRA, R., KONG, L.*, et al.* 2014. Gut-adipose tissue axis in hepatic fat accumulation in humans. *J Hepatol,* 61**,** 132-8.

NAVEAU, S., GAUDE, G., ASNACIOS, A., AGOSTINI, H., ABELLA, A., BARRI-OVA, N.*, et al.* 2009. Diagnostic and prognostic values of noninvasive biomarkers of fibrosis in patients with alcoholic liver disease. *Hepatology,* 49**,** 97-105.

OLEFSKY, J. M. & GLASS, C. K. 2010. Macrophages, inflammation, and insulin resistance. *Annu Rev Physiol,* 72**,** 219-46.

PEKKALA, S., MUNUKKA, E., KONG, L., POLLANEN, E., AUTIO, R., ROOS, C.*, et al.* 2015. Toll-like receptor 5 in obesity: The role of gut microbiota and adipose tissue inflammation. *Obesity (Silver Spring),* 23**,** 581-90.

PEREIRA, K., SALSAMENDI, J. & CASILLAS, J. 2015. The Global Nonalcoholic Fatty Liver Disease Epidemic: What a Radiologist Needs to Know. *J Clin Imaging Sci,* 5**,** 32.

PURI, P., BAILLIE, R. A., WIEST, M. M., MIRSHAHI, F., CHOUDHURY, J., CHEUNG, O.*, et al.* 2007. A lipidomic analysis of nonalcoholic fatty liver disease. *Hepatology,* 46**,** 1081-90.

QUEVRAIN, E., MAUBERT, M. A., MICHON, C., CHAIN, F., MARQUANT, R., TAILHADES, J.*, et al.* 2015. Identification of an anti-inflammatory protein from Faecalibacterium prausnitzii, a commensal bacterium deficient in Crohn's disease. *Gut*.

QUEVRAIN, E., MAUBERT, M. A., MICHON, C., CHAIN, F., MARQUANT, R., TAILHADES, J.*, et al.* 2016. Identification of an anti-inflammatory protein from Faecalibacterium prausnitzii, a commensal bacterium deficient in Crohn's disease. *Gut,* 65**,** 415-25.

RAVUSSIN, Y., KOREN, O., SPOR, A., LEDUC, C., GUTMAN, R., STOMBAUGH, J.*, et al.* 2012. Responses of gut microbiota to diet composition and weight loss in lean and obese mice. *Obesity (Silver Spring),* 20**,** 738-47.

ROGERS, C. Q., AJMO, J. M. & YOU, M. 2008. Adiponectin and alcoholic fatty liver disease. *IUBMB Life,* 60**,** 790-7.

ROSSI, O., VAN BERKEL, L. A., CHAIN, F., TANWEER KHAN, M., TAVERNE, N., SOKOL, H.*, et al.* 2016. Faecalibacterium prausnitzii A2-165 has a high capacity to induce IL-10 in human and murine dendritic cells and modulates T cell responses. *Sci Rep,* 6**,** 18507.

RYTKA, J. M., WUEEST, S., SCHOENLE, E. J. & KONRAD, D. 2011. The portal theory supported by venous drainage-selective fat transplantation. *Diabetes,* 60**,** 56-63.

SOKOL, H., PIGNEUR, B., WATTERLOT, L., LAKHDARI, O., BERMUDEZ-HUMARAN, L. G., GRATADOUX, J. J.*, et al.* 2008. Faecalibacterium prausnitzii is an anti-inflammatory commensal bacterium identified by gut microbiota analysis of Crohn disease patients. *Proc Natl Acad Sci U S A,* 105**,** 16731-6.

TAIRA, R., YAMAGUCHI, S., SHIMIZU, K., NAKAMURA, K., AYABE, T. & TAIRA, T. 2015. Bacterial cell wall components regulate adipokine secretion from visceral adipocytes. *J Clin Biochem Nutr,* 56**,** 149-54.

TAKAHASHI, Y., SOEJIMA, Y. & FUKUSATO, T. 2012. Animal models of nonalcoholic fatty liver disease/nonalcoholic steatohepatitis. *World J Gastroenterol,* 18**,** 2300-8.

TURNER, N., BRUCE, C. R., BEALE, S. M., HOEHN, K. L., SO, T., ROLPH, M. S.*, et al.* 2007. Excess lipid availability increases mitochondrial fatty acid oxidative capacity in muscle: evidence against a role for reduced fatty acid oxidation in lipid-induced insulin resistance in rodents. *Diabetes,* 56**,** 2085-92.

WANG, H. Y., DUCOMMUN, S., QUAN, C., XIE, B., LI, M., WASSERMAN, D. H.*, et al.* 2013. AS160 deficiency causes whole-body insulin resistance via composite effects in multiple tissues. *Biochem J,* 449**,** 479-89.

WESTON, C. J., SHEPHERD, E. L., CLARIDGE, L. C., RANTAKARI, P., CURBISHLEY, S. M., TOMLINSON, J. W., *et al.* 2015. Vascular adhesion protein-1 promotes liver inflammation and drives hepatic fibrosis. *J Clin Invest,* 125**,** 501-20.

VIDELA, L. A., RODRIGO, R., ARAYA, J. & PONIACHIK, J. 2004. Oxidative stress and depletion of hepatic long-chain polyunsaturated fatty acids may contribute to nonalcoholic fatty liver disease. *Free Radic Biol Med,* 37**,** 1499-507.

WILLIAMSON, D. L., LI, Z., TUDER, R. M., FEINSTEIN, E., KIMBALL, S. R. & DUNGAN, C. M. 2014. Altered nutrient response of mTORC1 as a result of changes in REDD1 expression: effect of obesity vs. REDD1 deficiency. *J Appl Physiol (1985),* 117**,** 246-56.

VIRTANEN, K. A., LONNROTH, P., PARKKOLA, R., PELTONIEMI, P., ASOLA, M., VILJANEN, T., *et al.* 2002. Glucose uptake and perfusion in subcutaneous and visceral adipose tissue during insulin stimulation in nonobese and obese humans. *J Clin Endocrinol Metab,* 87**,** 3902-10.

FIGURE LEGENDS

Figure 1. Faecalibacterium prausnitzii treatment decreases hepatic AST and ALT levels, fat content and improves histological changes caused by high-fat diet

The figure shows the effects of the treatments on A) hepatic AST and ALT levels, B) H&E, Oil Red O and α-smooth muscle actin (SMA) staining of the frozen liver sections. The SMA signal is high in vasculature of mice under high fat diet. The arrows point to the highly positive vessels (looking overexposed and seen as bright yellow) in a high fat diet mouse. The signal was weaker in other groups and the arrows point to those vessels as comparison (middle and bottom panels). Instead, the signal was weak outside the vasculature of the mice under high fat diet and hardly visible in other groups. Note that the exposure time was exactly the same in all cases. Scale bar 100 μm. C) total triglycerides and phospholipids contents.

All data are presented as mean ± SD. n was 4-6/group. The statistical significance was set to $p<0.05$ and the significant differences are presented with lines and * between the groups.

Figure 2. Faecalibacterium prausnitzii treatment enhances adiponectin signaling and lipid oxidation in liver

The figure shows the effects of the treatments on A) the expression of adiponectin receptor (*AdipoR*) mRNA, BD) the expression of citrate synthase (*CS*) mRNA, as well as C) the phosphorylation levels of acetyl coenzyme carboxylase (Acc) and D) the phosphorylation levels of AS160.

Figure 3. F. prausnitzii treatment increases adiponectin expression and insulin sensitivity, and decreases inflammation in the visceral adipose tissue

The figure shows the effects of the treatments on A) the expression of adiponectin (*AdipoQ*) mRNA, B) the visceral fat mass indicated in grams (g), C) the number of CD45-positive leukocytes in the histological samples/high power field and the histological stainings (the arrows point towards the CD45 positive brown cells), scale bar 100 μm, D) the expression of insulin receptor β (*IRβ*) mRNA, and E) the phosphorylation levels of hormone sensitive lipase (HSL)

All data are presented as mean ± SD. n was 4-6/group. The statistical significance was set to $p<0.05$ and the significant differences are presented with lines and * between the groups.

Figure 4. F. prausnitzii treatment decreases inflammation and affects the phosphorylation of the glucose uptake-related protein in the subcutaneous adipose tissue

The figure shows the effects of the treatments on A) the subcutaneous fat mass, B) the phosphorylation levels of glucose uptake-related AS160, and C) the number of CD45-positive leukocytes in the histological samples divided by the counted fields.

All data are presented as mean ± SD. n was 4-6/group. The statistical significance was set to $p<0.05$ and the significant differences are presented with lines and * between the groups.

Figure 5. F. prausnitzii treatment increases gastrocnemius muscle size and the expression of the mitochondrial respiratory chain protein ATP5A

The figure presents the effects of the treatments on A) the *gastrocnemius* muscle mass and, B) the expression of the subunits of the mitochondrial respiratory chain complexes.

All data are presented as mean ± SD. n was 4-6/group. The statistical significance was set to $p<0.05$ and the significant differences are presented with lines and * between the groups.

Figure 6. F. prausnitzii treatment changes the gut microbiota composition

A) Pre-treatment stool samples. No phylum level differences were seen between the treatment groups. The genus *Allobaculum* being higher in chow control mice than in HFD control and *F. prausnitzii* treated mice.
B) Post-treatment colon content samples. Compared to the HFD control group, the amount of phylum *Bacteroidetes* was significantly lower and the abundance of *Firmicutes* was significantly higher in the *F. prausnitzii*-treated mice. In addition, phylum *Cyanobacteria* was more abundant in Chow control mice than in HFD control and *F. prausnitzii* treated mice ($p<0.05$ for both).
The abundances of genera *Lactobacillus* and *Streptococcus* increased in *F. prausnitzii* treated mice compared to the HFD and normal chow controls. In addition, genus *Allobaculum,* which was not prevalent in the HFD controls, was highly abundant in the majority of the normal chow controls and in all *F. prausnitzii*-treated mice.

n was 3-5/group. The statistical significance was set to $p<0.05$ and the significant differences are presented with * next to the name of the bacteria.

709 TABLES

710

711

712

713 ***Table 1. Molar percentages of hepatic triacylglycerol (TAG), phospholipid (PL) and***
714 ***cholesteryl ester (CE) classes.***

715 All data are presented as mean ± SD. n was 4-6/group. The statistical significance was set to
716 $p<0.05$

TAG	**Control/HFD** mol % mean ± SD	**Control/Chow** mol % mean ± SD	***F. prausnitzii*/HFD** mol % mean ± SD	***p*- value Control/HFD vs Control/Chow**	***p*- value Control/HFD vs *F. prausnitzii*/HFD**	***p*- value Control/Chow vs *F. prausnitzii*/HFD**
14:0	0.44 ± 0.08	0.50 ± 0.09	0.46 ± 0.07	0.413	0.73	0.886
16:0	22.91 ± 1.52	19.27 ± 1.74	23.23 ± 1.12	0.063	1.00	**0.029**
16:1	2.44 ± 0.16	1.32 ± 0.46	2.10 ± 0.68	**0.016**	0.413	0.114
18:0	3.19 ± 0.29	1.12 ± 0.08	2.44 ± 0.26	**0.016**	**0.036**	0.057
18:1n-9	39.41 ± 0.72	60.86 ± 1.43	41.52 ± 2.46	**0.029**	0.686	**0.029**
18:2n-6	17.79 ± 0.43	4.14 ± 0.50	16.78 ± 1.65	**0.029**	0.686	**0.029**
18:3n-3	0.83 ± 0.12	0.18 ± 0.09	0.73 ± 0.07	**0.016**	0.393	0.057
18:3n-6	0.68 ± 0.15	0.13 ± 0.07	0.52 ± 0.09	**0.016**	0.111	**0.029**
20:1n-9	0.33 ± 0.03	0.64 ± 0.10	0.40 ± 0.07	**0.029**	0.200	**0.029**
20:2n-6	0.35 ± 0.03	0.54 ± 0.08	0.38 ± 0.04	**0.029**	0.343	0.057
20:3n-6	0.42 ± 0.16	0.22 ± 0.12	0.40 ± 0.06	0.111	0.571	0.229
20:4n-6	2.36 ± 0.18	0.57 ± 0.16	2.01 ± 0.18	**0.036**	**0.016**	0.057
20:5n-3	0.51 ± 0.01	0.12 ± 0.04	0.35 ± 0.01	**0.029**	**0.036**	0.057
22:6n-3	2.93 ±b 0.26	0.29 ± 0.07	2.12 ± 0.29	**0.016**	**0.036**	0.057
PL						
14:0	0.08 ± 0.01	0.08 ± 0.01	0.06 ± 0.01	0.556	0.063	**0.016**
16:0	21.71 ± 0.45	20.25 ± 0.73	20.30 ± 1.31	**0.008**	**0.008**	0.841
16:1	0.57 ± 0.06	2.03 ± 0.23	0.48 ± 0.09	**0.008**	0.190	**0.016**
18:0	17.04 ± 0.87	12.29 ± 0.72	17.97 ± 0.81	**0.008**	0.095	**0.008**
18:1n-9	9.18 ± 1.52	17.77 ± 0.81	8.63 ± 0.84	**0.008**	0.905	**0.016**
18:2n-6	11.34 ± 0.50	6.56 ± 0.43	10.87 ± 1.13	**0.008**	0.690	**0.008**
18:3n-3	0.08 ± 0.01	0.04 ± 0.00	0.07 ± 0.01	**0.016**	0.190	**0.008**
18:3n-6	0.18 ± 0.01	0.16 ± 0.03	0.14 ± 0.02	0.286	**0.032**	0.222
20:1n-9	0.24 ± 0.02	0.21 ± 0.04	0.11 ± 0.02	0.286	**0.029**	**0.016**
20:2n-6	0.07 ± 0.01	1.74 ± 0.60	0.28 ± 0.03	0.286	**0.029**	**0.016**
20:3n-6	0.74 ± 0.06	1.98 ± 0.27	1.09 ± 0.17	**0.016**	**0.016**	**0.008**
20:4n-6	20.04 ± 0.58	19.85 ± 1.19	21.18 ± 1.38	1.000	0.150	**0.008**
20:5n-3	0.31 ± 0.08	0.15 ± 0.02	0.27 ± 0.09	**0.008**	0.548	0.151
22:6n-3	14.01 ± 1.75	9.72 ± 0.49	13.88 ± 1.60	**0.008**	0.841	**0.008**

CE						
14:0	0.68 ± 0.05	0.57 ± 0.08	0.47 ± 0.10	0.057	**0.034**	0.157
16:0	23.96 ± 0.24	19.11 ± 1.73	22.10 ± 2.20	0.057	0.077	0.157
16:1	2.52 ± 0.26	6.83 ± 0.58	2.11 ± 0.56	**0.034**	0.248	**0.034**
18:0	2.6 ± 0.33	1.02 ± 0.17	2.46 ± 0.16	**0.034**	0.289	**0.050**
18:1n-9	37.60 ± 0.75	57.44 ± 0.88	43.20 ± 6.89	**0.050**	0.289	**0.034**
18:2n-6	16.36 ± 0.542	3.42 ± 0.64	13.33 ± 2.02	**0.050**	**0.050**	**0.050**
18:3n-3	0.79 ± 0.02	0.07 ± 0.01	0.45 ± 0.17	**0.050**	**0.050**	**0.050**
18:3n-6	0.60 ± 0.03	0.15 ± 0.04	0.42 ± 0.10	**0.034**	0.100	**0.050**
20:1n-9	0.48 ± 0.33	0.68 ± 0.11	0.62 ± 0.48	0.400	0.289	**0.050**
20:2n-6	0.043 ± 0.20	0.47 ± 0.08	0.34 ± 0.03	0.289	0.773	**0.034**
20:3n-6	0.42 ± 0.019	0.12 ± 0.03	0.46 ± 0.15	**0.034**	0.724	**0.050**
20:4n-6	2.15 ± 0.11	0.42 ± 0.17	1.67 ± 0.30	0.057	**0.021**	0.057
20:5n-3	0.42 ± 0.02	0.01 ± 0.00	0.22 ± 0.11	**0.050**	**0.050**	**0.050**
22:6n-3	2.51 ± 10.20	0.16 ± 0.05	1.73 ± 0.83	**0.034**	0.480	0.100

717

718

719

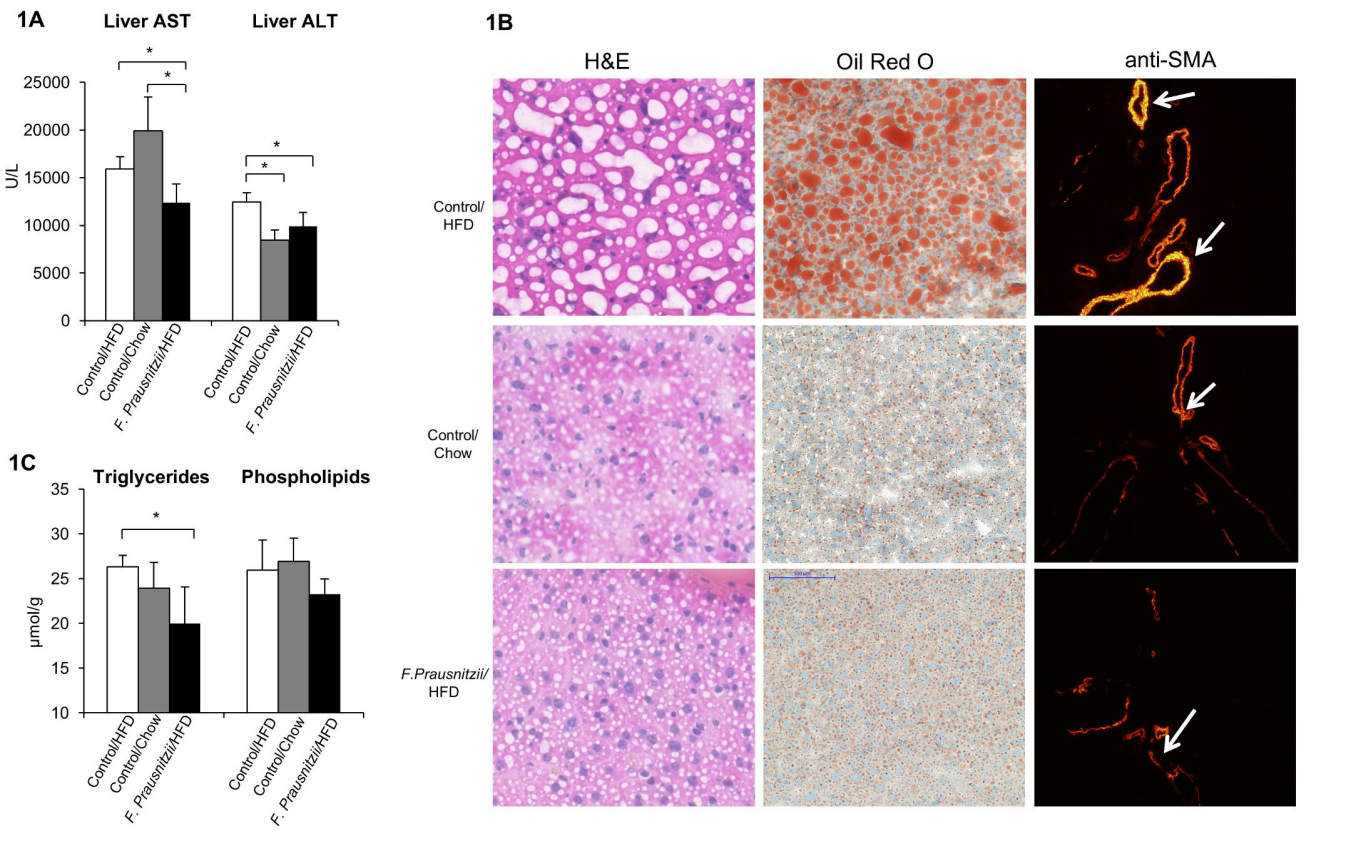
1A
Liver AST
Liver ALT
U/L
25000
20000
15000
10000
5000
0
*
*
*
*
Control/HFD
Control/Chow
F. Prausnitzii/HFD
Control/HFD
Control/Chow
F. Prausnitzii/HFD
1B
H&E
Oil Red O
anti-SMA
Control/ HFD
Control/ Chow
F.Prausnitzii/ HFD
1C
Triglycerides
Phospholipids
µmol/g
35
30
25
20
15
10
*
Control/HFD
Control/Chow
F. Prausnitzii/HFD
Control/HFD
Control/Chow
F. Prausnitzii/HFD

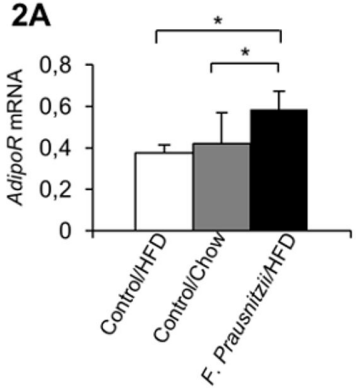
2A
AdipoR mRNA
0,8
0,6
0,4
0,2
0
*
*
Control/HFD
Control/Chow
F. Prausnitzii/HFD

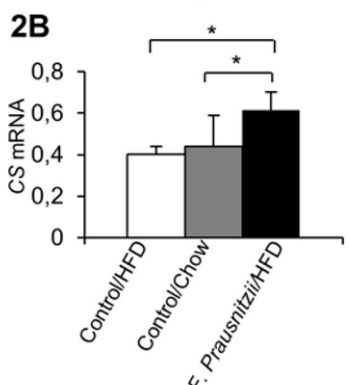
2B
CS mRNA
0,8
0,6
0,4
0,2
0
*
*
Control/HFD
Control/Chow
F. Prausnitzii/HFD

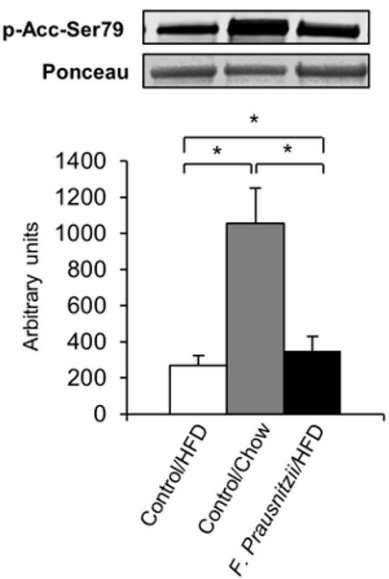
2C
p-Acc-Ser79
Ponceau
Arbitrary units
1400
1200
1000
800
600
400
200
0
*
*
*
Control/HFD
Control/Chow
F. Prausnitzii/HFD

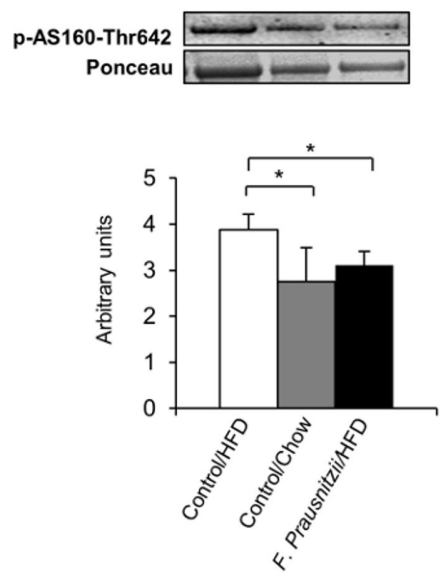
2D
p-AS160-Thr642
Ponceau
Arbitrary units
5
4
3
2
1
0
*
*
Control/HFD
Control/Chow
F. Prausnitzii/HFD

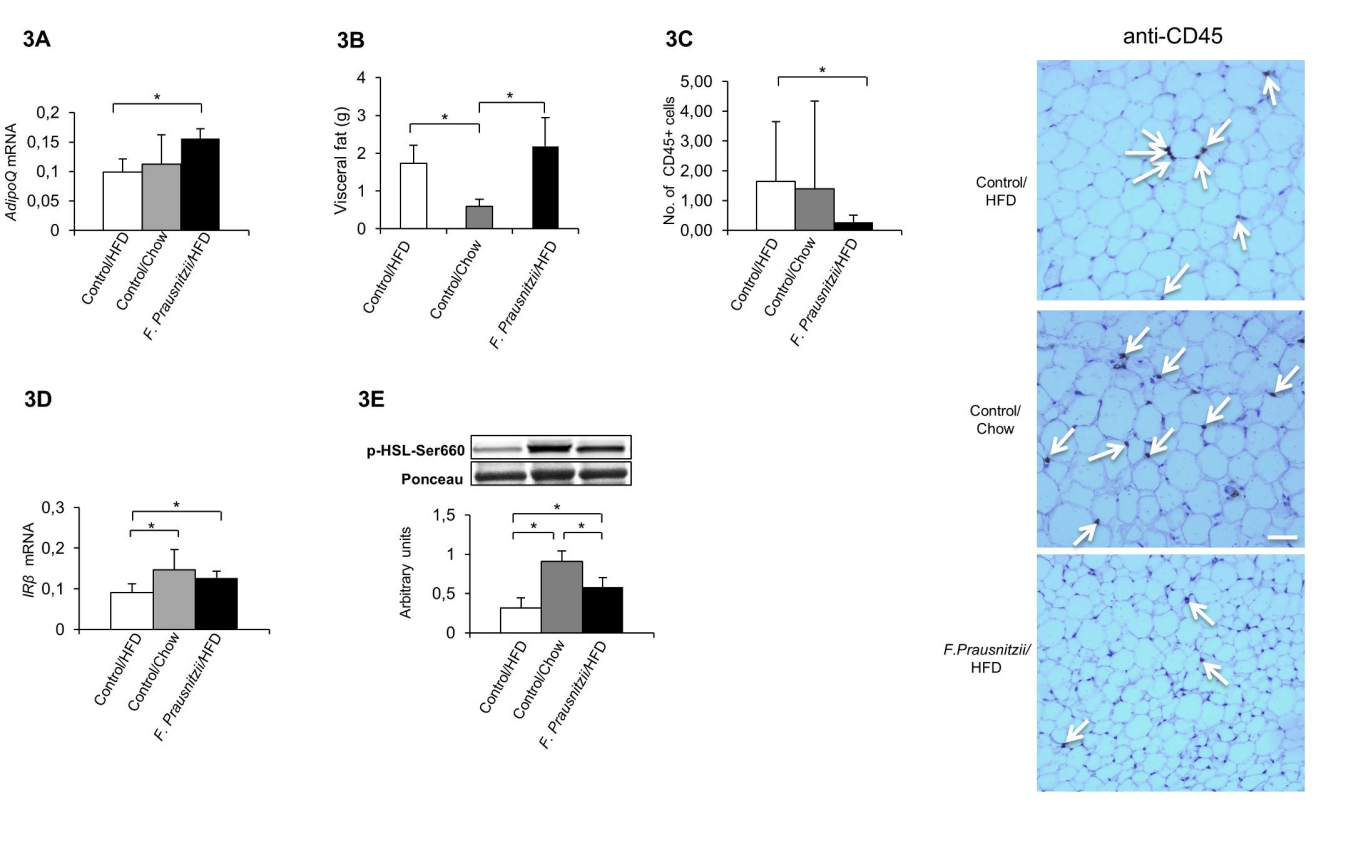
3A
AdipoQ mRNA
0,2
0,15
0,1
0,05
0
*
Control/HFD
Control/Chow
F. Prausnitzii/HFD
3B
Visceral fat (g)
4
3
2
1
0
*
*
Control/HFD
Control/Chow
F. Prausnitzii/HFD
3C
No. of CD45+ cells
5,00
4,00
3,00
2,00
1,00
0,00
*
Control/HFD
Control/Chow
F. Prausnitzii/HFD
anti-CD45
Control/ HFD
Control/ Chow
F.Prausnitzii/ HFD
3D
IRβ mRNA
0,3
0,2
0,1
0
*
*
Control/HFD
Control/Chow
F. Prausnitzii/HFD
3E
p-HSL-Ser660
Ponceau
Arbitrary units
1,5
1
0,5
0
*
*
*
Control/HFD
Control/Chow
F. Prausnitzii/HFD

4A

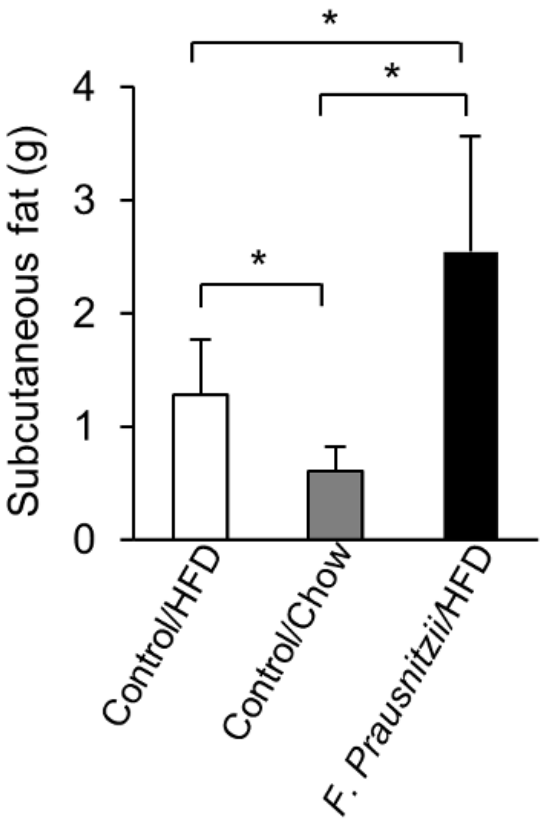
*
*
4
3
2
1
0
Subcutaneous fat (g)
Control/HFD
Control/Chow
F. Prausnitzii/HFD

4B

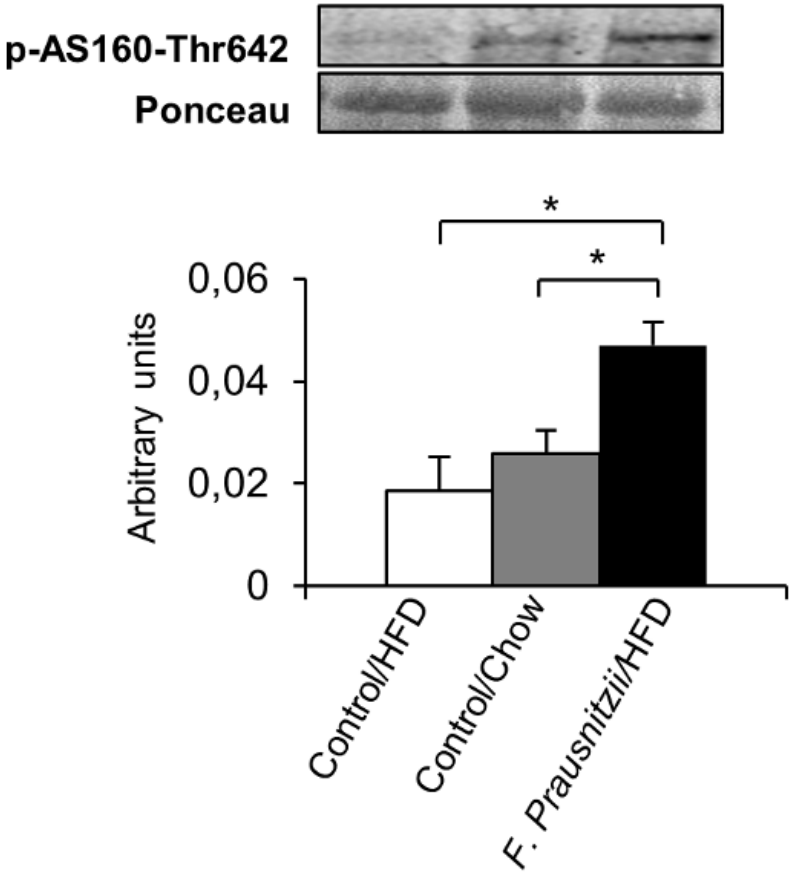
p-AS160-Thr642
Ponceau
*
*
0,06
0,04
0,02
0
Arbitrary units
Control/HFD
Control/Chow
F. Prausnitzii/HFD

4C

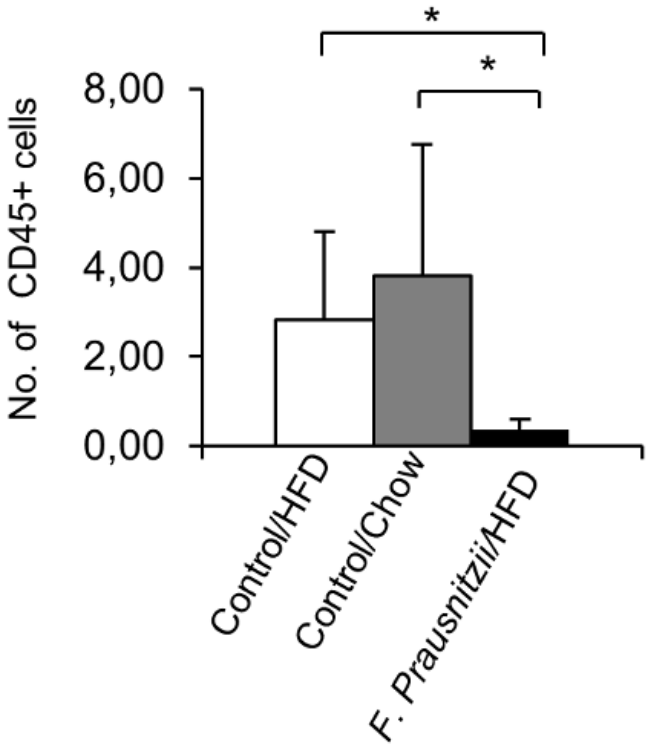
*
*
8,00
6,00
4,00
2,00
0,00
No. of CD45+ cells
Control/HFD
Control/Chow
F. Prausnitzii/HFD

5A

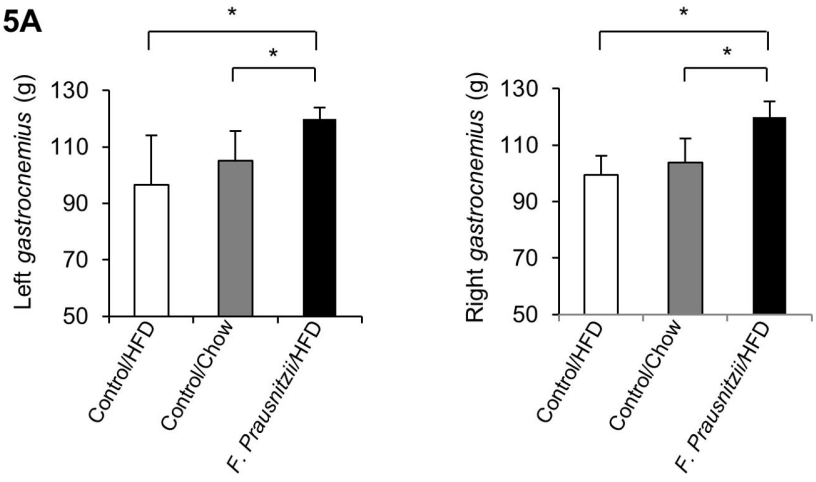
Left gastrocnemius (g)
130
110
90
70
50
*
*
Control/HFD
Control/Chow
F. Prausnitzii/HFD
Right gastrocnemius (g)
130
110
90
70
50
*
*
Control/HFD
Control/Chow
F. Prausnitzii/HFD

5B

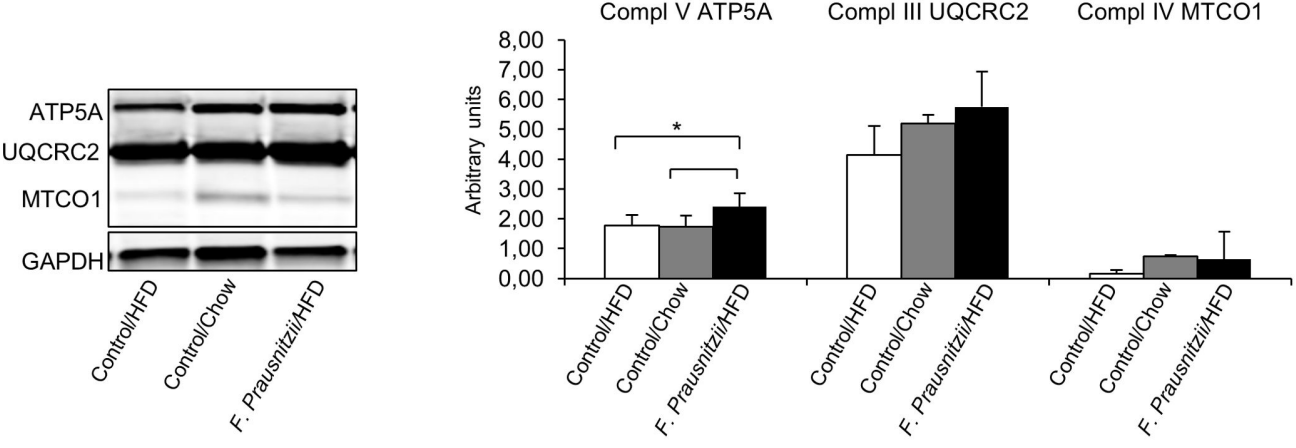
ATP5A
UQCRC2
MTCO1
GAPDH
Control/HFD
Control/Chow
F. Prausnitzii/HFD
Compl V ATP5A
Compl III UQCRC2
Compl IV MTCO1
Arbitrary units
8,00
7,00
6,00
5,00
4,00
3,00
2,00
1,00
0,00
*
Control/HFD
Control/Chow
F. Prausnitzii/HFD
Control/HFD
Control/Chow
F. Prausnitzii/HFD
Control/HFD
Control/Chow
F. Prausnitzii/HFD

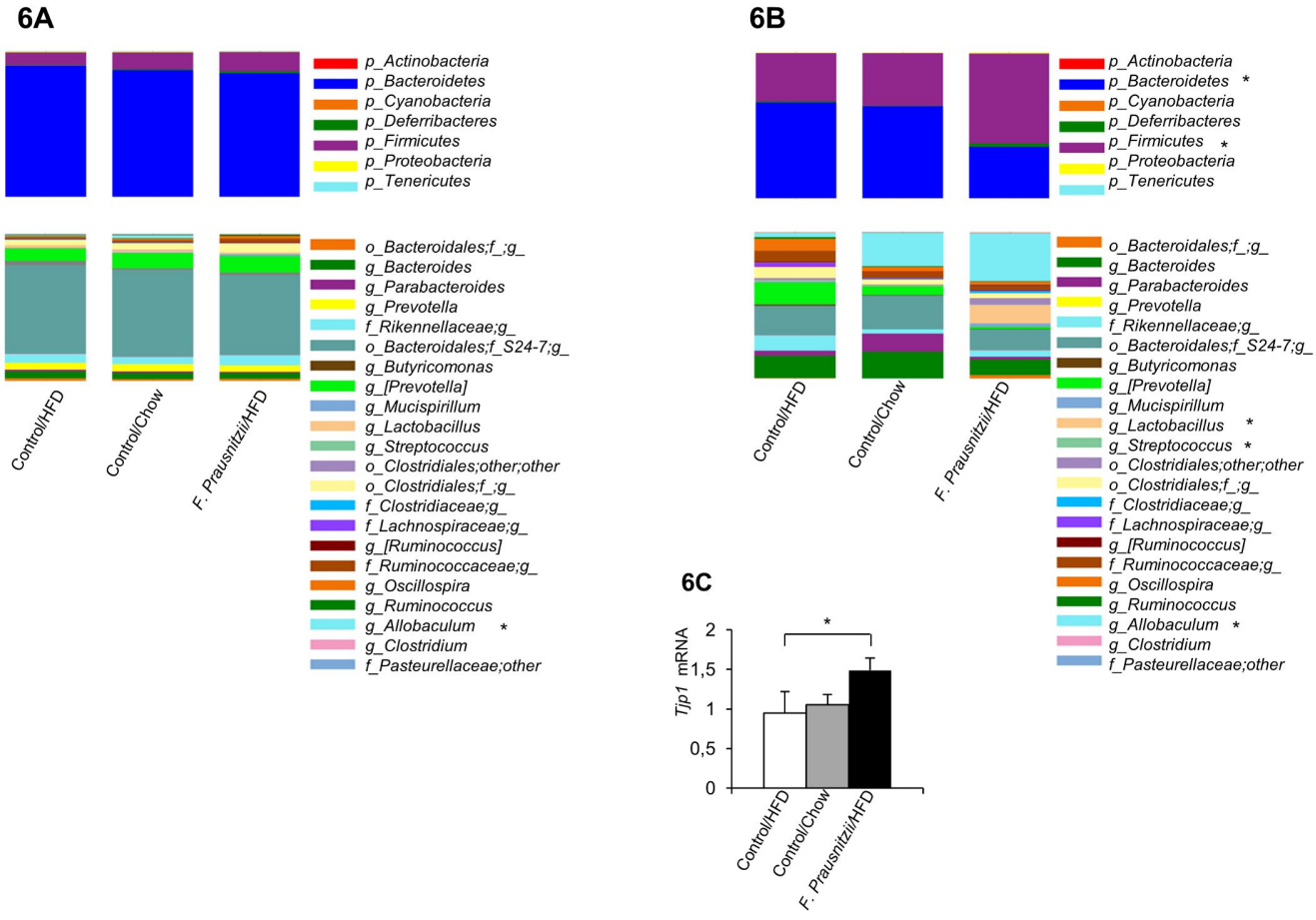
6A
p_Actinobacteria
p_Bacteroidetes
p_Cyanobacteria
p_Deferribacteres
p_Firmicutes
p_Proteobacteria
p_Tenericutes
o_Bacteroidales;f_;g_
g_Bacteroides
g_Parabacteroides
g_Prevotella
f_Rikennellaceae;g_
o_Bacteroidales;f_S24-7;g_
g_Butyricomonas
g_[Prevotella]
g_Mucispirillum
g_Lactobacillus
g_Streptococcus
o_Clostridiales;other;other
o_Clostridiales;f_;g_
f_Clostridiaceae;g_
f_Lachnospiraceae;g_
g_[Ruminococcus]
f_Ruminococcaceae;g_
g_Oscillospira
g_Ruminococcus
g_Allobaculum *
g_Clostridium
f_Pasteurellaceae;other
Control/HFD
Control/Chow
F. Prausnitzii/HFD
6B
p_Actinobacteria
p_Bacteroidetes *
p_Cyanobacteria
p_Deferribacteres
p_Firmicutes *
p_Proteobacteria
p_Tenericutes
o_Bacteroidales;f_;g_
g_Bacteroides
g_Parabacteroides
g_Prevotella
f_Rikennellaceae;g_
o_Bacteroidales;f_S24-7;g_
g_Butyricomonas
g_[Prevotella]
g_Mucispirillum
g_Lactobacillus *
g_Streptococcus *
o_Clostridiales;other;other
o_Clostridiales;f_;g_
f_Clostridiaceae;g_
f_Lachnospiraceae;g_
g_[Ruminococcus]
f_Ruminococcaceae;g_
g_Oscillospira
g_Ruminococcus
g_Allobaculum *
g_Clostridium
f_Pasteurellaceae;other
Control/HFD
Control/Chow
F. Prausnitzii/HFD
6C
Tjp1 mRNA
2
1,5
1
0,5
0
*
Control/HFD
Control/Chow
F. Prausnitzii/HFD